Available online at www.sciencedirect.com

ScienceDirect

Energy Procedia 53 (2014) 268 – 279

Energy Procedia

EERA DeepWind'2014, 11th Deep Sea Offshore Wind R&D Conference

A comparison on the dynamics of a floating vertical axis wind turbine on three different floating support structures

Michael Borg[a,]*, Maurizio Collu[a]

[a]*Cranfield University, Cranfield, MK43 0AL, United Kingdom*

Abstract

To increase the competitiveness of offshore wind energy in the global energy market, it is necessary to identify optimal offshore wind turbine configurations to deliver the lowest cost of energy. For deep waters where floating wind turbines are the feasible support structure option, the vertical axis wind turbine concept might prove to be one of these optimal configurations. This paper carries out a preliminary investigation into the dynamics of a vertical axis wind turbine coupled with three generic floating support structures originally intended for horizontal axis wind turbines. The modifications to the original characteristics of the support structures were kept to a minimum to illustrate the use of floating horizontal axis wind turbine platforms for floating vertical axis wind turbines Issues regarding the adequacy of the mooring systems are outlined and an overview of platform responses in a number of varying met-ocean conditions is presented and discussed.

Selection and peer-review under responsibility of SINTEF Energi AS

Keywords: VAWT; coupled dynamics; floaing wind turbine; support structures; mooring system

1. Introduction

As wind farms are pushed into deeper waters, the need for cost-effective solutions to extract energy from offshore wind is paramount. Whilst so far the optimal onshore wind turbine design, that is, the 3-bladed upwind horizontal axis wind turbine (HAWT), has been 'marinised' for use offshore, it may not be the optimal design for floating wind applications. One promising concept that may be more suitable for multi-megawatt scale floating offshore wind turbines (FOWTs) is the vertical axis wind turbine (VAWT). Using the FloVAWT (Floating VAWT) design tool

* Corresponding author.
E-mail address: m.borg@cranfield.ac.uk

Selection and peer-review under responsibility of SINTEF Energi AS
doi:10.1016/j.egypro.2014.07.236

currently being developed at Cranfield University as part of the EU FP7-H2Ocean project[†], this study focuses on investigating the dynamic behaviour of a typical multi-megawatt VAWT atop different support structures originally proposed by the FOWT industry for HAWTs. The paper is organized as follows; section 2 gives a brief description of the time-domain design tool used; section 3 outlines the three floating wind turbine systems studied; section 4 discusses some issues pertaining to the platform mooring systems; section 5 describes the loading conditions simulated; section 6 presents simulation results, analysis and interpretation; and section 7 provides some conclusions.

2. Numerical model description

The time-domain numerical tool used in this study is the FloVAWT design tool currently being developed at Cranfield University (Collu et al. [1; 2]) in the MATLAB/Simulink environment as part of the FP7-H2Ocena project to developed a novel combined floating wind-wave energy converter. Since no floating VAWT experimental data is publicly available, a code-to-code verification exercise was carried out in collaboration with researchers at the Norwegian University of Science and Technology, resulting in overall good agreement between codes (see Borg et al. [3]). Below follows a brief description of each FloVAWT module used in this study.

Aerodynamics: The aerodynamic model implemented to characterise the VAWT is the Double Multiple Streamtube (DMS) momentum model with a new velocity vector formulation (Collu et al. [2]) and modifications to include dynamic stall, tip and junction losses, 3D effects and tower shadow (Shires [4]). Validation of this model may be found in the work presented by Shires [4] and subsequently by Collu et al. [2].

Hydrodynamics: The hydrodynamic model is based on the Cummins equation and implemented using the Marine Systems Simulator Toolbox by Fossen and Perez [5], with a number of modifications tailored to floating VAWTs. Validation of this module was carried out for a number of floating platforms, including the GVA4000 and OC4 semi-submersible, as presented by Collu et al. [1; 2].

Inertial considerations: The focus of model development has so far been on interfacing aerodynamic and hydrodynamic modules and a structural model has not yet been developed for the design tool. Hence inertial effects due to the rotating rotor were explicitly defined to consider gyroscopic effects through an analytical formulation as developed by Blusseau and Patel [6] and highlighted by Collu et al. [1].

Mooring line dynamics: The mooring systems were represented by a linearized force-displacement relation in this study, as although a quasi-static catenary module has been developed (Collu et al.[2]), a dedicated module for tensioned moorings has not yet been developed. Hence to apply the same level of modeling across all three floating VAWTs analysed, the linearized force-displacement relation is considered.

3. Definition of floating wind turbine systems

In this study, the baseline 5MW DeepWind VAWT rotor developed by Vita [7] at the Technical University of Denmark is coupled with three floating support structures developed for the Offshore Code Comparison Collaboration (OC3), Offshore Code Comparison Collaboration, Continuation (OC4) and DeepCwind projects. Note that modifications to the original characteristics of the support structures were kept to a minimum to illustrate the use of floating HAWT platforms for floating VAWTs. The turbine and three support structures are briefly outlined in the following sections.

[†] www.h2ocean-project.eu

3.1. Vertical axis wind turbine

The 5MW VAWT baseline design developed by Vita [7] in relation to the FP7-DeepWind project is of the curved-blade, Darrieus type, as depicted in Fig.1. Whilst this is not the optimized version as presented by Paulsen et al. [8], at the time of conducting this study all relevant details were only available for the baseline design. Table 1 presents the main geometric, inertial and operational characteristics of the turbine.

3.2. Spar

The spar design used in this study is the same used in the OC3 Phase IV project [9] with a catenary mooring system rather than the taut mooring system used in the DeepCwind project [10]. Whilst the geometry has remained the same, inertial characteristics have been modified to account for the VAWT inertia. Fig. 2a presents a conceptual view of the floating VAWT spar and Table 2 highlights the main characteristics of the *total* floating wind turbine system.

Table 1 – Rotor main characteristics

Rotor height, root-to-root (m)	129.56
Rotor radius (m)	63.74
Chord (m)	7.45
Airfoil section	NACA0018
Total mass, including tower and generator (kg)	844226
Centre of gravity, from tower base (m)	67.4
Rated power (MW)	5.0
Rated wind speed at 79.78m above MSL (m/s)	14
Rated rotational speed (rpm)	5.26

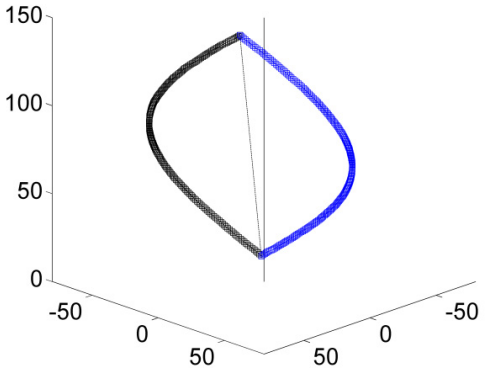

Figure 1 - Rotor geometry visualisation

3.3. Semi-submersible

The semi-submersible design is based on that used in the OC4 Phase II project [11] and also tested in the DeepCwind project [10]. To maintain the same draft specified for the floating HAWT, the ballast was rearranged to accommodate the VAWT, as described by Wang et al. [12]. This floating wind turbine has also been used in a floating VAWT code verification study by Borg et al. [3]. Fig. 2b presents a conceptual view of the floating VAWT semi-submersible and Table 2 highlights the main characteristics of the *total* floating wind turbine system.

3.4. Tension-leg-platform (TLP)

The TLP design utilized is based on the design by University of Maine for the DeepCwind project [13; 14]. The inertial characteristics of the VAWT were combined with those of the TLP. The current VAWT has a larger mass that the HAWT used in DeepCwind, and the pre-tensioning of the tendons was adjusted to maintain the same draft as the original floating HAWT. Fig. 2c presents a conceptual view of the floating VAWT TLP and Table 2 highlights the main characteristics of the *total* floating wind turbine system.

4. Degrees of freedom

One prominent difference between HAWTs and VAWTs is the nature of the generator torque generated. Whilst for a floating HAWT the torque generated is about the roll axis and is accommodated by the inherent platform restoring stability, the highly oscillatory torque generated by a VAWT imparted on the support structure is about the yaw axis, with only the mooring system capable of accommodating this excitation. Hence the design criteria for the mooring system of a floating HAWT and a floating VAWT are significantly different. For the three support

structures originally designed for HAWTs considered here, only the semi-submersible mooring system can accommodate the VAWT rotor torque without catastrophic failure of the system.

The spar mooring system does not have a large enough yaw stiffness to sustain station-keeping of the platform. This is due to the moment arms of mooring fairlead connections. To illustrate this, Fig. 3 presents a sample time history of the yaw motion of the spar platform with original mooring system operating at rated conditions. As can be seen, the platform motion quickly spirals out of control, leading to catastrophic failure.

Whilst a solution to this would be to extend the moment arm of the fairleads through the use of torque arms, as done in the DeepWind project [7], for this study the yaw degree of freedom (DOF) was disabled. This was done so that the impact of such a 5MW VAWT can be investigated when using a support structure originally intended for a 5MW HAWT.

Table 2 - Floating wind turbine systems main characteristics

	Spar	Semi-sub	TLP
Draft (m)	120	20	30
Mass (tonnes)	8125.2	14108	1505.8
Centre of Gravity (CG), from keel (m)	45.37	11.07	64.1
Radius of gyration about CG , roll (m)	30.11	30.59	66.88
Radius of gyration about CG, pitch (m)	29.01	29.97	64.13
Radius of gyration about CG, yaw (m)	8.83	29.91	19.85

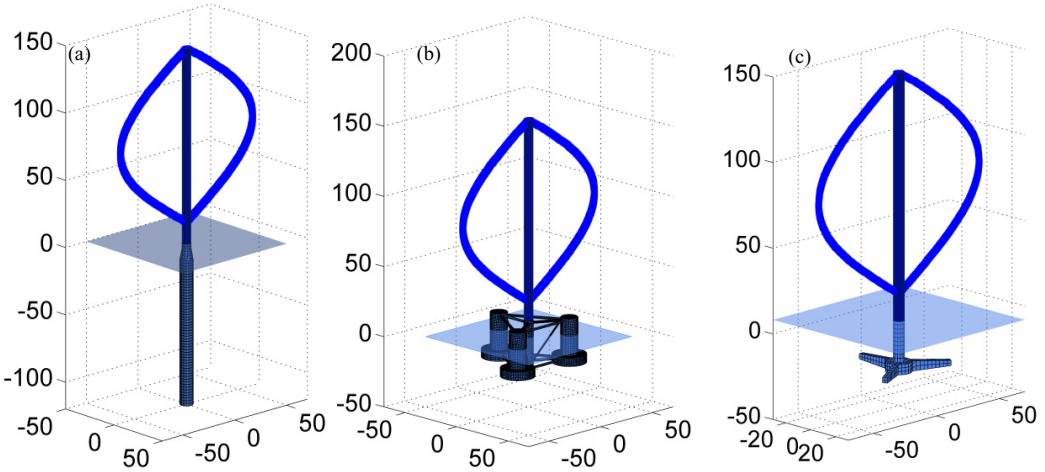

Figure 2- Visualisation of floating wind turbines, (a) Spar; (b) Semi-submersible; (c) TLP

The impact on the other DOFs of disabling yaw is minimal; as the submerged spar structure is symmetrical in both the surge-heave plane and sway-heave plane, any yaw motion would not augment wave excitation forces in other DOFs and there are no inertial couplings between yaw and other DOFs. Also radiation force couplings between yaw and sway, and yaw and roll are five orders of magnitude lower when compared to sway-sway and roll-roll radiation force couplings.

In the case of the TLP, the mooring system surge and sway restoring stiffnesses cannot sustain the VAWT forces, with the TLP proceeding to exhibit ringing behaviour at above rated wind conditions[‡]. Fig. 4 depicts a plan view of the motion of the TLP on the sea surface in operating in met-ocean conditions with a wind speed of 21.8 m/s

[‡] VAWT aerodynamic forces oscillate at a frequency equivalent to the number of blades multiplied by the rotational speed, which is relatively high for multi-megawatt VAWTs with respect to 1st order wave frequencies. In this study this aerodynamic frequency is 1.1 rad/s.

(equivalent to LC4.5 in Table 6 below). As can be seen, the platform is uninhibited in moving on the sea surface and unrealistic displacements are reached within a short period of time. Whilst the linearized mooring model does not capture the nonlinear characteristics of the mooring lines, particularly at large displacements where surge and sway stiffness would be augmented due to inclination of the mooring tendons, this aspect is still an issue in the technical feasibility of floating VAWT TLPs.

Hence for the purpose of this study the surge and sway degrees of freedom are disabled. The impact on other DOFs could be noticeable:

- surge and sway are coupled through mooring restoring stiffnesses with pitch and roll, respectively;
- surge-pitch and sway-roll radiation force couplings are only one order of magnitude lower than pitch-pitch and roll-roll radiation couplings, respectively;
- in the coordinate system framework within FloVAWT, surge-pitch and sway-roll inertial couplings are present (FOWT centre of gravity is not at the origin if the coordinate system);
- surge and sway motion would augment relative air flow through the VAWT, modifying aerodynamic forces on the FOWT.

Following these statements, the TLP response amplitude operators (RAOs) in heave and pitch were constructed for wave-only conditions with and without the surge and sway DOFs disabled. Whilst the heave RAO had no appreciable difference, the pitch RAO was significantly affected due to the strong surge-pitch mooring stiffness that induced a peak in response at the surge-pitch coupling natural frequency, as shown in Fig. 5. On this basis the TLP was not considered in the simulation studies presented in sections 5 and 6. This emphasizes the need to develop different station-keeping design criteria for floating VAWTs and alternative mooring systems that fulfill such criteria.

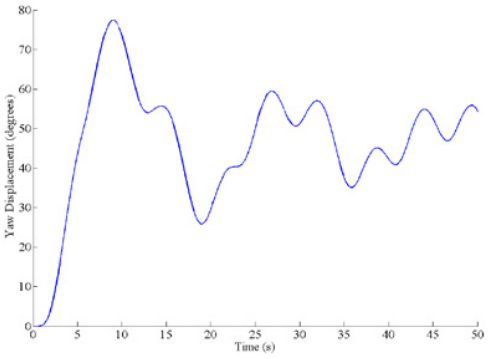

Figure 3 - Spar yaw instability

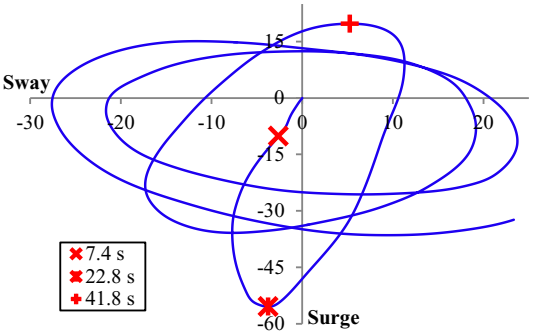

Figure 4 - Plan view of TLP surge-sway instability, symbols mark instances in simulation

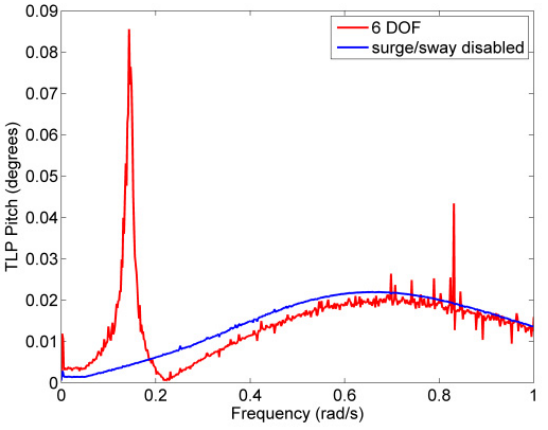

Figure 5 - Effect on TLP pitch RAO of disabling surge and sway DOFs

5. Loading conditions & environmental conditions

5.1. Loading conditions

A series of load cases were set up to assess a number of different aspects of the three floating wind turbine systems:

- Load Case 1: free decay simulations with turbine in parked condition to determine platform natural frequencies and damping ratios
- Load Case 2: white noise incident wave simulations with no wind to obtain motion responses of platforms
- Load Case 3: wind only simulations to assess impact of aerodynamic forces on platform motion
- Load Case 4: realistic met-ocean conditions to assess stochastic responses of each FOWT.

Note that in this study, the turbine rotational speed was kept constant at 5.26rpm throughout all turbine-operating simulations. Tables 3 through 6 present the relevant parameters for load cases 1 to 4, respectively.

5.2. Environmental conditions

5.2.1. Atmospheric & Wind Conditions

The air density was fixed at 1.225kg/m^3 and the dynamic viscosity was fixed at 1.789 x 10^{-5}kg/m s. For load cases with steady wind conditions, a vertical wind profile is applied based on the equation:

$$U_i = U_{ref}\left(Z_i / Z_{ref}\right)^{\alpha} \qquad (1)$$

where U_{ref} is the reference velocity at hub height, z_{ref} is the hub height and α is the power law exponent. For this study z_{ref} = 79.78 metres above mean sea level and α = 0.14 (according to IEC 61400-3).

Table 3 - Load case 1 parameters: free decay simulations

		Initial conditions		Simulation Length (s)		Time step (s)
		Spar	Semi-sub	Spar	Semi-sub	
LC1.1	Surge	+12m	+12m	1200	1200	0.1
LC1.2	Heave	+6m	+6m	150	150	0.1
LC1.3	Pitch	+5deg	+8deg	300	300	0.1
LC1.4	Yaw	N/A	+8deg	N/A	900	0.1

Table 4 - Load case 2 parameters: white noise wave spectrum simulation

	No.of wave components	Length (s)	Time step (s)
LC2.1	800	3600	0.1

Table 5 - Load case 3 parameters: wind only simulations

	Wind Condition	U_{ref} (m/s)	Simulation Length (s)	Time step (s)
LC3.1	Cut-in	5	1800	0.1
LC3.2	Below-rated	9	1800	0.1
LC3.3	Rated	14	1800	0.1
LC3.4	Above-rated	18	1800	0.1
LC3.5	Cut-off	25	1800	0.1

Table 6 - Load case 4 parameters: realistic met-ocean conditions simulations

	U_{ref} (m/s)	H_s (m)	T_p (s)	Simulation Length (s)	Time step (s)
LC4.1	7.3	2.1	9.74	3600	0.1
LC4.2	8.9	2.88	9.98	3600	0.1
LC4.3	14.24	3.62	10.29	3600	0.1
LC4.4	16.1	5.32	11.06	3600	0.1
LC4.5	21.8	6.02	11.38	3600	0.1

5.2.2. Sea & wave conditions

For sub-load cases with irregular unidirectional waves, the mean wave direction was aligned with the wind, coinciding with the x-axis and the water depth was set to 320 metres for the spar and 200 metres for the other two platforms. The JONSWAP sea spectrum was applied and the significant wave height and peak spectral period for each sub-load case are specified in Table 6.

6. Results & discussion

6.1. System identification

The free decay simulations carried out in load case 1 were used to deduce the natural periods and damping ratios of the three platforms in the relevant DOFs. Note that for DOFs disabled, as discussed in section 4, free decay simulations were not carried out (cf. Table 3). The natural periods and damping ratios obtained are presented in Table 7.

Table 7 - Platform natural periods and damping rations obtained from free decay simulations

	Natural period (s)				Damping ratio			
	Surge	Heave	Pitch	Yaw	Surge	Heave	Pitch	Yaw
Spar	137.7	31.7	41.0	N/A	0.050	0.060	0.057	N/A
Semi-submersible	112.6	17.5	29.0	80.2	0.066	0.097	0.050	0.037

In surge, both the spar and semi-submersible have natural periods exceeding 110 seconds due to the low surge restoring stiffness of the catenary mooring systems employed. In heave, the spar natural period (31.7 seconds) is on the upper limit of the period range (5-30 seconds) of first order wave excitation forces for most operating sea states. The semi-submersible on the other hand has a heave natural period (17.5 seconds) that is well within the wave excitation range, indicating significant platform motions particularly in more severe met-ocean conditions. The TLP heave natural period is very short at 1.07 seconds, well above environmental load excitation periods. A similar conclusion is reached for pitch, with the semi-submersible more likely to have larger motions than the other platforms.

6.2. Response amplitude operators

Fig. 6 presents the surge and heave RAOs of the two platforms. Fig. 7 presents the pitch RAO of the three platforms. These RAOs were obtained through unidirectional white noise simulations (LC2). The double-peak characteristic of the semi-submersible is predicted across all DOFs, although is not very visible in surge. In pitch, the spar peak is response is rather large at almost eight degrees per unit wave height. This is mainly due to the linear viscous model applied in FloVAWT, which could possibly require more calibration to achieve more realistic RAOs.

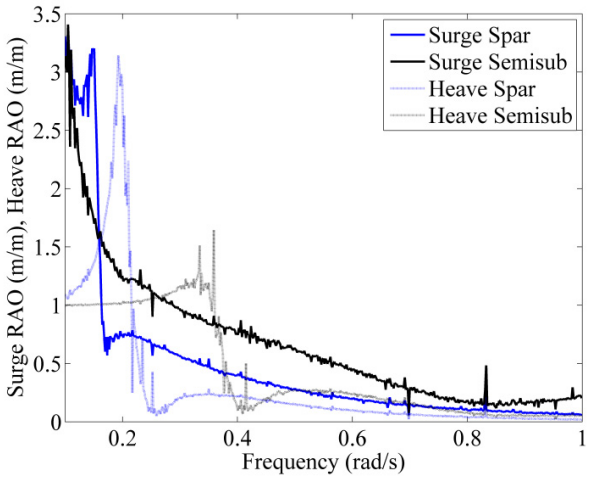

Figure 6 - Platform Surge and Heave RAOs

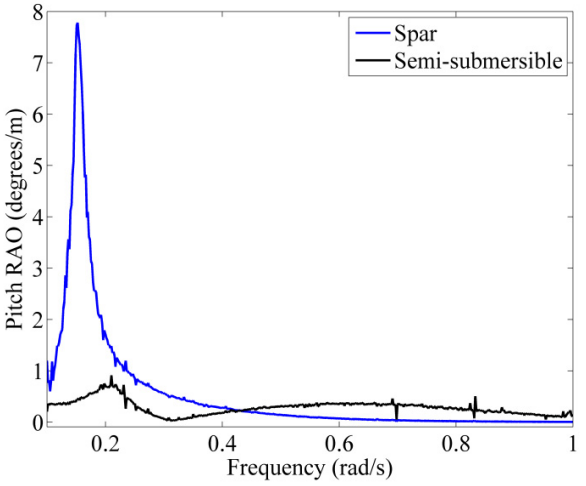

Figure 7 - Platform Pitch RAOs

6.3. Wind only simulations

Figs. 8 through 11 present the mean displacements of the two platforms in surge, heave, pitch and yaw, respectively, with error bars representing standard deviation for wind only simulations (LC3). Platform data is not presented in DOFs that have been disabled, as outlined earlier. In surge, both the spar and semi-submersible follow the same trend in mean displacements, both at below-rated (LC3.1 and 3.2) and at above-rated wind speeds (LC3.4 and 3.5). The standard deviation, or variability, of spar surge motion is significantly less than of the semi-submersible, due to the different amounts of viscous damping, mooring stiffnesses and natural frequencies between the two platforms.

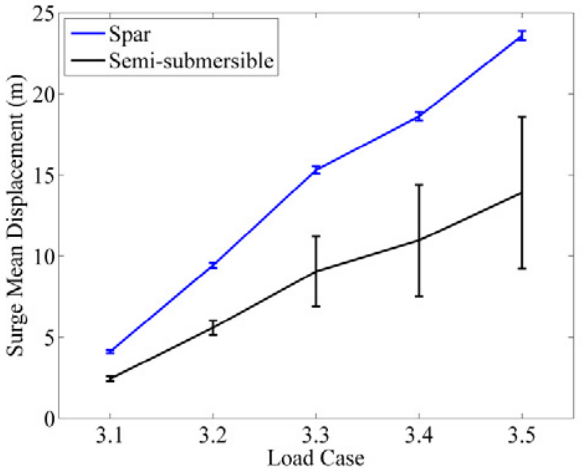

Figure 8 - LC3 Surge mean displacements & standard deviations

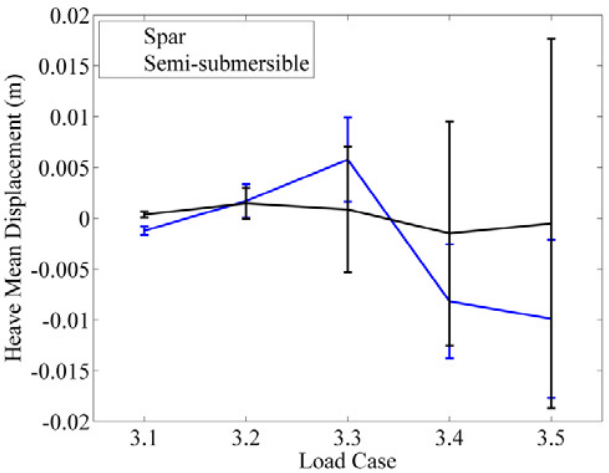

Figure 9 - LC3 Heave mean displacements & standard deviations

Once again in heave, the spar and semi-submersible follow similar trends in mean displacement, albeit the spar exhibits large amplitudes due to the significantly lower hydrostatic heave restoring stiffness as compared to the semi-submersible. The ‘uplifting’ of the semi-submersible in heave occurs as the mean aerodynamic heave force is in the upward direction. The aerodynamic heave force is a function of the platform roll and pitch motion, and the azimuth angle of the turbine with respect to the incoming wind. This combination of factors may lead to the aerodynamic heave force ‘uplifting’ the semi-submersible by a few millimetres, although since the design tool used is in the preliminary stages of development, this may not occur in reality. The change in gradient direction at above-rated wind speeds (LC3.4 and 3.5) is due to the change in the aerodynamic operating regime of the VAWT.

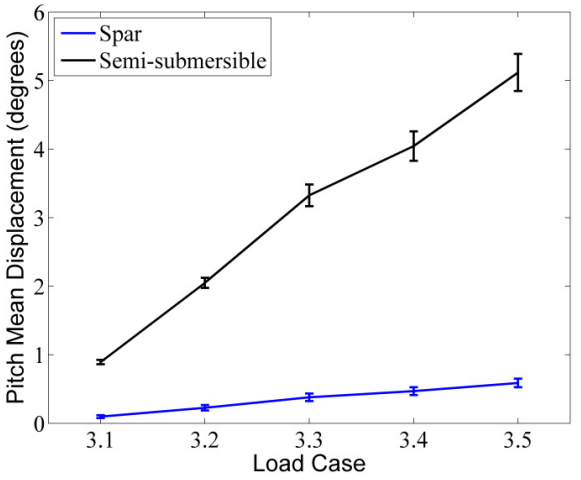

Figure 10 - LC3 Pitch Mean displacements & standard deviations

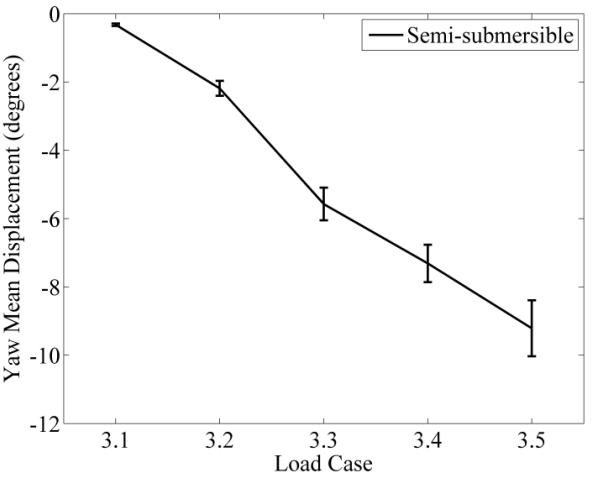

Figure 11 - LC3 Yaw mean displacements & standard deviations

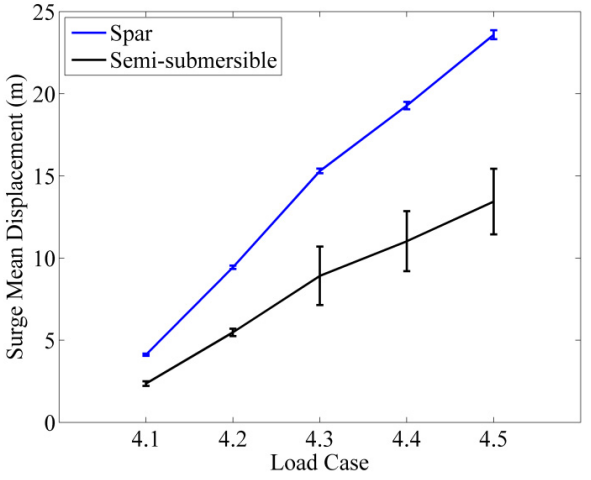

Figure 12 - LC4 Surge mean displacements & standard deviations

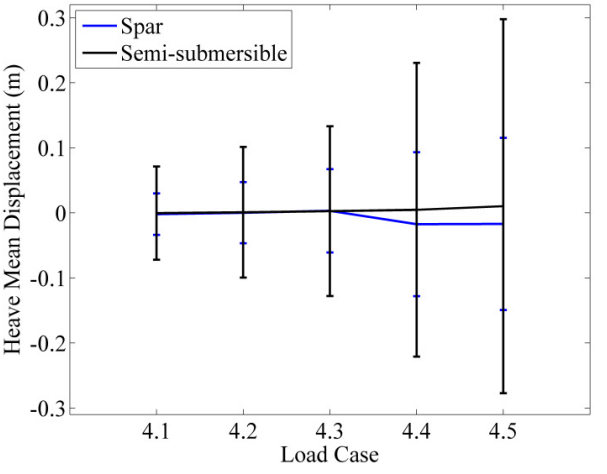

Figure 13 - LC4 Heave mean displacements & standard deviations

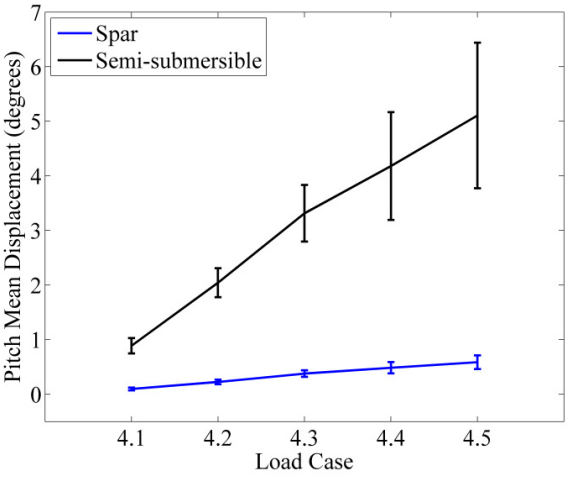

Figure 14 - LC4 Pitch Mean displacements & standard deviations

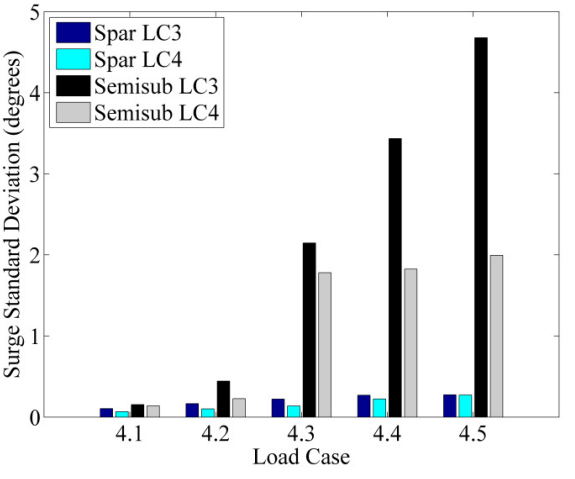

Figure 15 - Comparison of LC3 & LC4 surge standard deviations

At above-rated wind speeds dynamic stall becomes predominant, and coupled with platform-induced turbine velocities, can significantly alter the profile of aerodynamic forces. Notwithstanding, the mean displacements are on the order of one centimetre, and hence are not significant.

In pitch, the trend is similar to mean surge displacements, albeit that in this DOF the semisubmersible produced significantly larger amplitudes. This is due to the fact that since the spar mooring attachment points are found towards the bottom of the 120 metre submerged length, there is a large moment arm for the translational mooring restoring forces. In yaw, the aerodynamic torque is the only predominant load, leading to mean yaw displacements of the semi-submersible being a function of this torque and yaw mooring stiffness. One can observe that the semi-submersible mean yaw displacement is significant, particularly in severe met-ocean conditions, which would exacerbate wave excitation forces in other DOFs as the platform is at an angle to the incoming irregular waves. Anyway, it has to be considered that the semi-submersible here used has been designed for an HAWT, and therefore for a much lower yaw moment.

6.4. Met-ocean simulations

Figs. 12 through 14 present the mean displacements of the two platforms in surge, heave and pitch, respectively, with error bars representing standard deviation for met-ocean simulations (LC4). Platform data is not presented in DOFs that have been disabled, as outlined earlier. Similar observations are made as in wind only simulations, with significant differences mainly in predicted standard deviations. Only in heave was there a significant change in the mean displacement trends. The model predicts that the wave heave excitation dampens the effect of aerodynamic forces in heave, which is reasonable, as the irregular motion induced by wave excitation would disrupt the regular platform motion that otherwise occurs in wind only simulations. The wave heave excitation forces are also significantly larger than the aerodynamic heave forces, which also contributes to dampening of the aerodynamic effect. This regular motion would induce periodic increased VAWT relative velocities and hence increase aerodynamic forces. Since in wind only conditions the platform dominantly oscillates at the forcing frequency (i.e. aerodynamic force oscillatory frequency), this would generate platform-induced velocities at frequencies favourable to increased aerodynamic forces.

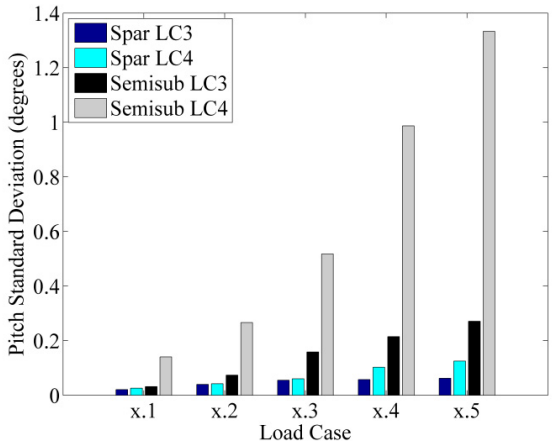

Figure 16- Comparison of LC3 & LC4 pitch standard deviations

6.5. Wind only versus met-ocean platform responses

Following on the discussion of platform responses in met-ocean conditions, it is interesting to further compare responses in wind only and met-ocean simulations. Figs. 15 and 16 present a comparison of the standard deviations for wind only (LC3) and met-ocean (LC4) simulations for surge and pitch respectively. An interesting observation is that whilst the presence of waves reduced the variability of surge motion for both spar and semi-submersible, the variability of pitch motion increased for both these platforms. The semi-submersible pitch motion standard deviation

increases by a factor of between 3 and 5 in met-ocean conditions as compared to wind only simulations., whilst much smaller increases are predicted for the other two platforms.

7. Conclusions

An investigation into the feasibility of using floating support structures originally designed for HAWTs with a comparable VAWT was carried out. A spar, semi-submersible and tension-leg-platform originally designed for HAWTs were coupled with the DeepWind 5MW baseline VAWT design. Issues pertaining to the inadequacy of the original mooring systems were presented, illustrating the differences in mooring design requirements for VAWTs as compared to HAWTs. The spar was found not to be able to sustain the aerodynamic loads in yaw and the TLP mooring system could not sufficiently restrain the platform in surge and sway. These observations highlight the need to develop specific design criteria for the station-keeping of floating VAWTs, taking into account the additional required dynamic restraints in surge, sway and yaw. Since there is a critical surge-pitch coupling for the TLP, the TLP could not be appropriately simulated and hence the current design was excluded from further simulations. A number of varying environmental conditions were simulated using the FloVAWT design tool and an overview of the motion responses of the spar and semi-submersible was presented, illustrating the interaction of aerodynamic and hydrodynamic loads on platform motions. The results indicated that whilst the floating support structures can sufficiently support the VAWT, the mooring systems need to be redesigned particularly to adequately restrain the floating VAWT in surge, sway and yaw. Future work will investigate new design criteria and configurations for floating VAWTs.

Acknowledgements

The research leading to these results has been performed in the frame of the H2OCEAN project (**www.h2ocean-project.eu**) and has received funding from the European Union Seventh Framework Programme (FP7/2007-2013) under grant agreement nº 288145. It reflects only the views of the author(s) and the European Union is not liable for any use that may be made of the information contained herein.

References

[1] Collu, M., Borg, M., Shires, A. and Brennan, F. P. (2013), "Progress on the development of a coupled model of dynamics for floating offshore vertical axis wind turbines", *Proceedings of the ASME 2013 32nd International Conference on Ocean, Offshore and Arctic Engineering,* 9-14 June, 2013, Nantes, France, ASME.

[2] Collu, M., Borg, M., Shires, A., Rizzo, N. F. and Lupi, E. (2014), "Further progresses on the development of a coupled model of dynamics for floating offshore VAWTs", *ASME 33rd International Conference on Ocean, Offshore and Arctic Engineering,* 8-13 June 2014, San Francisco, USA.

[3] Borg, M., Wang, K., Collu, M. and Moan, T. (2014), "Comparison of two coupled model of dynamics for offshore floating vertical axis wind turbines (VAWT)", *ASME 33rd International Conference on Ocean, Offshore and Arctic Engineering,* 8-13 June, 2014, San Francisco, USA.

[4] Shires, A. (2013), "Development and Evaluation of an Aerodynamic Model for a Novel Vertical Axis Wind Turbine Concept", *Energies,* vol. 6, no. 5, pp. 2501-2520.

[5] Fossen, T. I. and Perez, T. *, MSS. Marine Systems Simulator (2010)*, available at: http://www.marinecontrol.org (accessed 16.04.2012).

[6] Blusseau, P. and Patel, M. H. (2012), "Gyroscopic effects on a large vertical axis wind turbine mounted on a floating structure", *Renewable Energy*.

[7] Vita, L. (2011), *Offshore floating vertical axis wind turbines with rotating platform* (Ph.D. thesis), Technical University of Denmark, Roskilde, Denmark.

[8] Paulsen, U. S., Madsen, H. A., Hattel, J. H., Baran, I. and Nielsen, P. H. (2013), "Design Optimization of a 5 MW Floating Offshore Vertical-axis Wind Turbine", *Energy Procedia,* vol. 35, pp. 22-32.

[9] Jonkman, J. and Musial, W. (2010), *Offshore Code Comparison (OC3) for IEA Task 23 Offshore Wind Technology and Deployment,* NREL/TP-5000-48191, NREL, Colorado.

[10] Robertson, A., Jonkman, J. M., Masciola, M., Molta, P., Goupee, A. J., Coulling, A. J., Prowell, I. and Browning, J. (2013), "Summary of Conclusions and Recommendations Drawn from the DeepCWind Scaled Floating Offshore Wind System Test Campaign", *ASME 2013 32nd International Conference on Ocean, Offshore and Arctic Engineering,* 9-14 June 2013, Nantes, France.

[11] Robertson, A., Jonkman, J., Musial, W., Vorpahl, F. and Popko, W. (2013), "Offshore Code Comparison Collaboration, Continuation: Phase II Results of a Floating Semisubmersible Wind System", *EWEA Offshore 2013,* 19-21 November, 2013, Frankfurt, Germany.

[12] Wang, K., Moan, T. and Hansen, M. O. L. (2013), "A method for modeling of floating vertical axis wind turbine", *Proceedings of the ASME 2013 32nd International Conference on Ocean, Offshore and Arctic Engineering,* 9-14 June, 2013, Nantes, France, ASME.

[13] Stewart, G. M., Lackner, M., Robertson, A., Jonkman, J. and Goupee, A. J. (2012), "Calibration and Validation of a FAST Floating Wind Turbine Model of the DeepCwind Scaled Tension-Leg Platform", *22nd International Offshore and Polar Engineering Conference,* 17-22 June, 2012, Rhodes, Greece, ISOPE.

[14] Goupee, A. J., Koo, B. J., Lambrakos, K. F. and Kimball, R. W. (2012), "Model tests for three floating wind turbine concepts", *Offshore Technology Conference,* 30 April-3 May 2012, Texas.